Detecting Chronic Vascular Damage with Attention-Guided Neural System

Muhammad Zubair Khan[1], Yugyung Lee[2], Arslan Munir[3] and Muazzam Ali Khan[4]

***Abstract*—The retinal vasculature has a vital role in predicting chronic diabetic and hypertensive retinopathy. Recently, the advent of deep learning algorithms has brought a revolution in ocular disease prediction. The researchers frequently design complex and intricate techniques to efficiently segment vessels, micro-vessels and achieve better response on publicly available benchmark datasets. This article has designed an attention-guided neural system to extract vascular tree and distinguish it in arteries and veins. The proposed learning protocol with a minimalist approach can compete with state-of-the-art work without a performance compromise. Our method has achieved a promising response on numerous retinal image datasets. The pitfall of previously proposed work is also addressed through the self-defined assessment criteria. The in-depth analysis highlights that the underlying problem is unsolved for unseen data with different distribution than training. Our method is cross-validated to report the performance loss by keeping diversity in data selection. The technique is further applied for the arteries and veins extraction. Our effort can be adapted as an efficient vision-critical platform to scan and localize retinal damage and diagnose the disease symptoms early to prevent vision impairment.**

***Index Terms*—deep learning, diabetic retinopathy, fundus image, hypertensive retinopathy, vessels segmentation.**

I. Introduction

Deep learning has received great appreciation from the AI community for a diverse range of applications. The main application includes image segmentation, classification, detection, restoration, and registration. The appearance of intelligence and efficient deep learning algorithms has revolutionized healthcare diagnostics. The core idea is to extract valuable features, anatomical structures, and corresponding regions of interest for early disease prediction [1]. The underlying article emphasized the application of deep learning for ocular disease prediction. It is found that many ocular and systemic diseases manifest themselves in the retina. The retinal image analysis can uncover the symptoms of many sight-threatening diseases like diabetic retinopathy (DR) and hypertensive retinopathy (HR) for restraining vision loss [2]. The DR is common in people facing diabetes. It weakens the inner surface of vessels and causes vascular occlusion with an excessive amount of blood sugar. It may transform into neovascularization in an advanced stage by producing new fragile micro-vessels that eventually cuts off the blood supply to nourish the retina. Similarly, in HR, chronic hypertension causes vessels to become thick and fragile and prevent blood from reaching the retina. The condition is referred to as arterial and venous occlusion. The extended force in arteries and veins produces vessel rupture, and eventually, blood and other fluids leak into the retina. The people with HR are potentially at a high risk of stroke and cardiac arrest. Typically during retinopathy examination, the subject pupils are dilated with special eye drops followed by injecting fluorescein into the body to capture DR and HR symptoms. The process is painful and error-prone, especially in the early stages. The underlying article has proposed a method for automated retinopathy (DR, HR) detection to help ophthalmologists in examining patients facing chronic diabetes and hypertension. Our method can be deployed as an assistive tool and play a vital part in preventing vision impairment.

A. Related Work

A dual-residual stream-based semantic model is developed in [3] for HR and DR diagnosis. It comprises internal and outer residual skip-paths to assure feature re-use and produce direct spatial edge information. Pires *et al.* developed a multi-scale convolution network with robust feature-extractor and data augmentation techniques for data-driven DR analysis [4]. [5] used image-level annotations to detect lesions for screening DR. Shankar *et al.* performed histogram-based segmentation with SDL model to extract potential regions [6]. The method classified mid and small-sized vessels by iteratively traversing the range of potential solutions. A method proposed in [7] has developed a bi-modular clinical decision system for vessels and optic nerve head analysis. The first module used a support vector machine with RBF kernel for A/V classification and ratio calculation, whereas, the second module performed analysis to detect the symptoms of papilledema. A multi-layered convolutional architecture with deep residual learning network is developed to detect HR-related ocular disease [8].

In [9], the authors designed a method to find the impact of deep learning in predicting hypertension, hyperglycemia, and dyslipidemia. The article [10] analyzed graphs extracted from vascular tree to classify in arteries and veins. The decision is made through graph nodes and graph links. In [11], a pixel classification with inter-subject normalization and intra-image regularization is used for A/V classification. The discriminating properties are captured using first and second-order texture features. The authors in [12] developed the topological graph-theoretic paradigm to discriminate arteries from veins.

[1]Muhammad Zubair Khan, School of Computing and Engineering, University of Missouri-Kansas City, Kansas City, USA (mkzb3@mail.umkc.edu)

[2]Yugyung Lee, School of Computing and Engineering, University of Missouri-Kansas City, Kansas City, USA (leeyu@umkc.edu)

[3]Arslan Munir, Department of Computer Science, Kansas State University, Manhattan, USA (amunir@ksu.edu)

[4]Muazzam Ali Khan, Department of Computer Science, Quaid-i-Azam University, Islamabad, Pakistan (muazzam.khattak@qau.edu.pk)

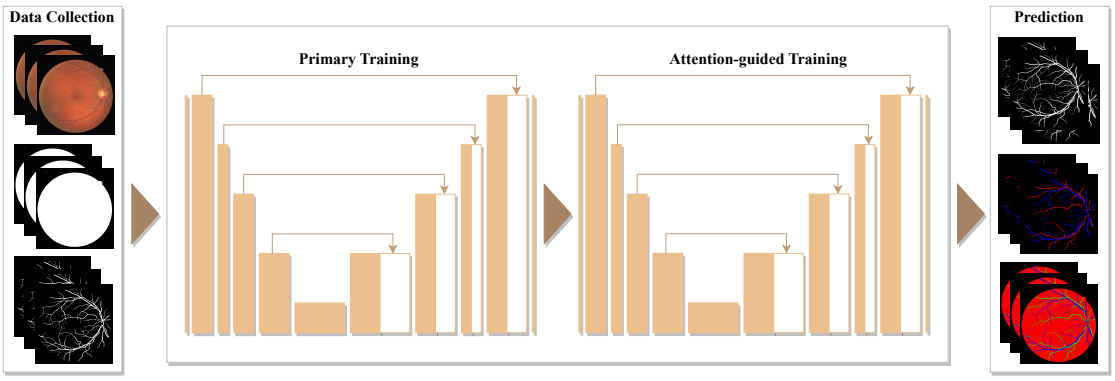

Fig. 1. The proposed attention-guided neural architecture to extract vascular tree, and differentiate retinal arteries from veins.

The U-Net architecture in [13] has used an encoder-decoder path with data augmentation to helps extract better feature representations with a limited amount of data. [14] integrated CRU with U-Net for capturing long dependencies and prevent vanishing gradient problem. [15] presented a context encoder network to preserve spatial information with dense atrous convolution and residual multi-kernel pooling. Oktay *et al.* introduced attention U-Net with a chain of convolutions and attention gates for extracting local and global feature representations [16]. [17] proposed UNet++ for semantic and instance segmentation. It is a multi-depth U-Net architecture with a novel pruning method for rapid inferencing. The IterNet architecture is presented in [18]. It has used a weight-sharing feature. Li *et al.* [19] developed SeqNet for segmentation and classification of vessels into arteries and veins.

B. Motivation and Contributions

The principal motivation behind this effort is to reveal that the vessel extraction task, even with simple architectural design, can compete with state-of-the-art work without performance compromise and show that the model experiences the worst response when tested with unseen data distribution. These facts forced us to make the following contributions:

1) We have developed a minimalistic attention-guided neural system for vessels and micro-vessels extraction to early detect the retinal damage caused by chronic diabetic and hypertensive retinopathy.
2) We defined model assessment criteria to overcome the shortcomings of the work previously proposed and verified our method with seven distinct fundus image datasets, publicly available with different resolutions, capturing angles, and focal points.
3) We conducted a cross-data experiment to prove that the performance of a model degrades when trained on one dataset and tested for other with different distribution.

II. Proposed Methodology

In this article, a deep attention guided neural architecture is designed, shown in Fig. 1. The network is defined in two halves. The first portion extracts the retinal vessels that are used by the second part as an input attention map to focus more on the local regions of interest. The training protocol described in Algorithm 1 is identical for all datasets used in our experiment. The standard data augmentation technique is applied on resized fundus images for producing additional synthetic data to avoid data scarcity. The architecture contains bi-phase encoding decoding structure. The depth increases through encoding and reduces as it passes through the decoding module. In contrast, the input dimension drops in the contraction path to function around key feature representations using max-pool operation; however, it gets back to its original shape with transpose convolution in the expansion path. The experiment has performed 4000 iterations by adjusting the number of cycles separately for each dataset. Every cycle is ex-

Algorithm 1 Learning Protocol

Input: Fundus Images (X,Y)
Output: Model $(\hat{m})$ that produces segmentation maps

Start
$l = [\varphi]$
X = Array$[x_1, x_2, \ldots, x_n]$
function data_train$(\mathbb{I}_{rgb})$
  for (x_i in range X) **do**
    d_i = Invoke weget(x_i)
    l.append(d_i)
    for ($\forall d$ in l) **do**
      Process d to produce file in CSV format
      Resize each sample in nxn dimension
      Perform image augmentation
    foreach (cycle in range $1-k$) **do**
      for ($\forall$batch in d_i) **do**
        Train model(m) for t epochs
        Update parameters(Θ) of m
        if (loss is constant for η epochs) **then**
          Upgrade learning_rate(λ) until 10^{-8}
        else
          Continue()
  return $(\hat{m})$
End

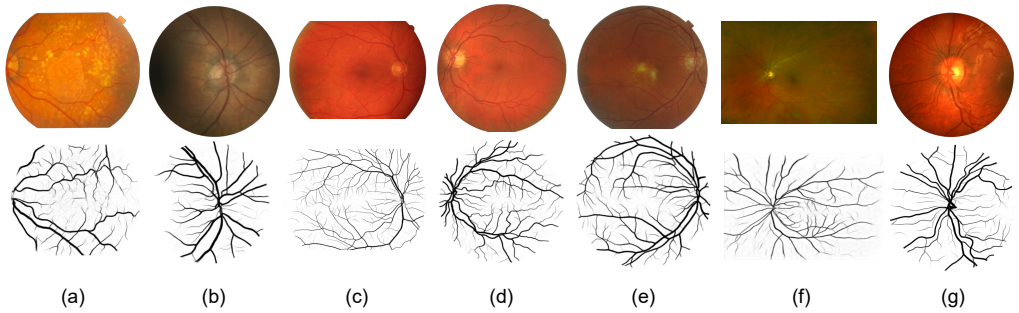

Fig. 2. Predictions on benchmark fundus image dataset. (a) STARE, (b) LES-AV, (c) HRF, (d) DRIVE, (e) DR-HAGIS, (f) AV-WIDE, (g) CHASEDB.

ecuted for 50 epochs with a constant batch-size of 4 and ReLU activation function. The cross-entropy loss function and Adam optimizer are used to minimize the cost of predictions, given by $\Delta\theta = -\lambda\hat{m}_t/\sqrt{\hat{v}_t + \varepsilon}$ where, $\hat{m}_t = m_t/(1-\beta_1^t)$ and $\hat{v}_t = v_t/(1-\beta_2^t)$ with $(\beta_1 = 0.9, \beta_2 = 0.999)$. The learning rate (λ) is initialized with $\lambda = 10^{-2}$ and gradually changed using cosine-law until approaches to $\lambda = 10^{-8}$. The network is assessed by excluding insignificant pixels outside the field-of-view with a negligible likelihood of being a vessel. The experiment made a decision of train/test split based on the presence of official data partitioning. In datasets without any visible split, we used previous literature to conduct a least favorable split in contrast to applying leave-one-out and multi-fold cross-validation strategies. A cross-data performance is reported for multiple retinal image datasets without any preprocessing and hyperparameter tuning. It helped prevent undermining the service of our approach for extracting retinal vasculature and differentiating arteries from veins in 2D imaging environment.

III. Experimentation and Results

A. Data and System Configuration

In a designed experiment, we have acquired data from multiple resources. The network is trained on three publicly available fundus image datasets DRIVE [20], HRF [21], and CHASEDB [22]. The DRIVE dataset comes with a standard train/test split; however, for the other two datasets, we used the partitioning strategy defined in [23]. In an experiment, 15 images from HRF and 8 images of CHASEDB are used for model training and validation. The remaining images are kept for testing. The cross-data examination is performed using four additional datasets, namely STARE [24], DR-HAGIS [25], AV-WIDE [26], and LES-AV [27]. The data came in different resolutions and image quality, captured under diverse luminance conditions. The system configured an 8^{th} generation intel processor with 16 GB primary memory and the NVIDIA 1070 GPU operated with 64-bit Windows operating system.

B. Evaluation and Cross-data Analysis

The proposed method performance is primarily evaluated through DICE and AUC metrics and results are provided in Table III. It is compared with multiple vessel segmentation techniques published recently for catering to a similar problem. When we observed our method, it is found that it surpasses by a massive margin to most of previously proposed work with least number of parameters. It is significant to mention that the proposed method with less complex end-to-end image-based architecture has achieved promising response for both vessels and A/V segmentation. The utility of a method can only be concluded if it is exhaustively tested on data different from the training resource. In order to justify this element, we performed a cross-data experiment, shown in Fig. 2. The model trained on the DRIVE dataset produced segmentations for six other fundus image datasets discussed in the previous section, including the unseen DRIVE test-set. Similarly, the process is repeated for CHASEDB and HRF datasets. The performance is analyzed and cross-data results are reported in Table I and Table II. The method is also applied for A/V segmentation. It classified every image pixel as artery, vein, or background pixel. The model trained on DRIVE is tested with DRIVE, HRF, and LES-AV datasets. The results are provided in Table III and illustrated in Fig. 4. It is found from an exhaustive analysis that the test sets with similar distribution, quality, and dimension to the training set have shown excellent response. Nonetheless, the performance degrades for the data with a different arrangement, depicted in Fig. 3. The worst response of HRF and DR-HAGIS is due to the higher image resolution than DRIVE and CHASEDB. Similarly, AV-WIDE has ultra-widefield images that capture the retina at a different angle. Also, the LES-AV images are more focused to the optic-disc region than a macula. However, the STARE, CHASEDB, and DRIVE are close in nature and centered across macula, sustaining excellent response in the cross-validation process.

TABLE I
TRAINING, VALIDATION AND TESTING RESPONSE OF PROPOSED METHOD.

Dataset	Accuracy	Specificity	Sensitivity	AUC	DICE
DRIVE	0.9579	0.9759	0.8339	0.9829	0.8337
	0.9517	0.9614	0.8823	0.9838	0.8168
	0.9555	0.9720	0.8419	0.9809	0.8281
CHASEDB	0.9752	0.9861	0.8872	0.9938	0.8876
	0.9675	0.9848	0.8300	0.9877	0.8514
	0.9630	0.9746	0.8535	0.9846	0.8164
HRF	0.9674	0.9814	0.8238	0.9854	0.8174
	0.9676	0.9816	0.8194	0.9863	0.8134
	0.9650	0.9808	0.8103	0.9828	0.8116

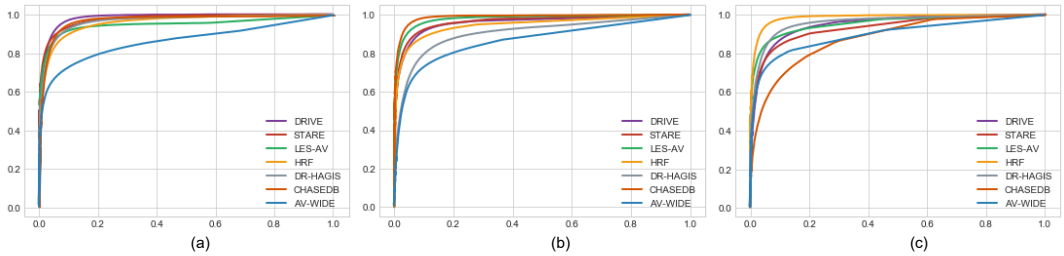

Fig. 3. The ROC plots of our method trained on (a) DRIVE, (b) CHASEDB, (c) HRF and evaluated for all acquired benchmark datasets.

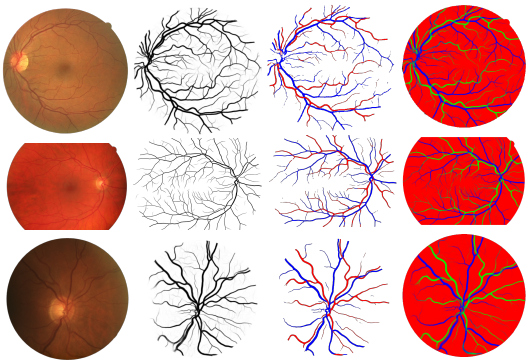

Fig. 4. Segmentation of arteries and veins. Top-to-bottom sequence depicts the prediction results obtained from DRIVE, HRF and LES-AV datasets.

TABLE II
CROSS-DATA EXPERIMENT OF AN ARCHITECTURE APPLIED FOR DRIVE, CHASEDB AND HRF DATASETS.

Training	Testing	Accuracy	Specificity	Sensitivity	AUC	DICE
DRIVE	CHASEDB	0.9449	0.9526	0.8759	0.9741	0.7618
	HRF	0.9312	0.9391	0.8528	0.9603	0.6937
	STARE	0.9462	0.9539	0.8791	0.9760	0.7714
	DR-HAGIS	0.9439	0.9508	0.8518	0.9672	0.6808
	AV-WIDE	0.9482	0.9716	0.6095	0.8624	0.6038
	LES-AV	0.9509	0.9627	0.8394	0.9496	0.7657
CHASEDB	DRIVE	0.9435	0.9880	0.6359	0.9586	0.7401
	HRF	0.9523	0.9718	0.7575	0.9454	0.7436
	STARE	0.9557	0.9866	0.6872	0.9634	0.7622
	DR-HAGIS	0.9015	0.9109	0.7774	0.9048	0.5259
	AV-WIDE	0.9416	0.9708	0.5201	0.8653	0.5357
	LES-AV	0.9618	0.9730	0.8551	0.9797	0.8105
HRF	DRIVE	0.9224	0.9881	0.6982	0.9477	0.6441
	CHASEDB	0.9151	0.9762	0.6884	0.8799	0.6385
	STARE	0.9354	0.9767	0.6023	0.9350	0.6626
	DR-HAGIS	0.9456	0.9568	0.7978	0.9600	0.6733
	AV-WIDE	0.9525	0.9877	0.6003	0.8971	0.6505
	LES-AV	0.9531	0.9770	0.6371	0.9538	0.6863

IV. Conclusion and Future Works

The article developed an attention-guided network to extract vascular tree, arteries, and veins. The idea behind this work is to promote a system that early examines the variations and damage in vessels caused by retinopathy. The recent effort has over-complicated the system architectures by searching for absolute novelty only to accumulate small performance growth. It is observed that a simple architecture, if appropriately developed, can significantly handle the problems for which complex solutions are defined. Additionally, considering inappropriate data distribution can inflate metrics and raise a wrong impression of a problem being solved. Often, the performance of a model trained on one dataset quickly diminishes when tested for distinct data. To analyze this fact, we have exhaustively evaluated our model on multiple datasets. In the future, this problem would be enhanced with inter-domain adaptation and feature ensembling techniques.

TABLE III
COMPARISON OF THE PROPOSED METHOD WITH OTHER TECHNIQUES, (∗) REPRESENTS AV EXTRACTION ONLY.

Dataset	DRIVE		CHASEDB/LES-AV*		HRF	
Method/Metric	DICE	AUC	DICE	AUC	DICE	AUC
Zhang [28]	–	0.9636	–	0.9606	–	0.9608
Liskowski [29]	–	0.9790	–	0.9845	–	–
Fu [30]	0.7875	0.9404	0.7549	0.9482	–	–
Gu [31]	0.7886	–	0.7202	–	0.7749	–
Orlando [32]	0.7857	0.9507	0.7332	0.9524	0.7158	0.9524
Yan [33]	0.8183	0.9752	–	0.9781	0.7814	–
Wang [34]	0.8093	–	0.7809	–	0.7731	–
Alom [35]	–	0.9784	–	0.9815	–	–
Shin [36]	0.8263	0.9801	0.8034	0.9830	0.8151	0.9838
Zhuang [37]	–	0.9793	–	0.9839	–	–
Laibacher [23]	0.8091	0.9714	0.8006	0.9703	0.7814	–
Mou [38]	–	0.9796	–	0.9812	–	–
Zhuo [39]	0.8163	0.9754	–	–	–	–
Zhao [40]	0.8229	–	–	–	0.7731	–
Liu [41]	–	0.9798	–	–	–	–
Galdran [42]*	0.9631	–	0.9659	–	–	–
Hemelings [43]*	0.9671	–	–	–	0.9688	–
AGNA−VT [Ours]	0.8281	0.9809	0.8164	0.9846	0.8116	0.9828
AGNA−AV [Ours]*	0.9687	–	0.9665	–	0.9693	–

V. Acknowledgment

The work is funded by the Balaji K. Memorial grant and School of Graduate Studies, UMKC. The responsibility of the research work is on the primary author and does not represent any view from the funding authorities.

References

[1] M. Z. Khan, M. K. Gajendran, Y. Lee, and M. A. Khan, "Deep neural architectures for medical image semantic segmentation: Review," *IEEE Access*, vol. 9, pp. 83 002–83 024, 2021.

[2] M. Z. Khan and Y. Lee, "Screening fundus images to extract multiple ocular features: A unified modeling approach," in *2021 IEEE EMBS International Conference on Biomedical and Health Informatics (BHI)*, 2021, pp. 1–5.

[3] M. Arsalan, M. Owais, T. Mahmood, S. W. Cho, and K. R. Park, "Aiding the diagnosis of diabetic and hypertensive retinopathy using artificial intelligence-based semantic segmentation," *Journal of clinical medicine*, vol. 8, no. 9, p. 1446, 2019.

[4] R. Pires, S. Avila, J. Wainer, E. Valle, M. D. Abramoff, and A. Rocha, "A data-driven approach to referable diabetic retinopathy detection," *Artificial intelligence in medicine*, vol. 96, pp. 93–106, 2019.

[5] G. Quellec, K. Charrière, Y. Boudi, B. Cochener, and M. Lamard, "Deep image mining for diabetic retinopathy screening," *Medical image analysis*, vol. 39, pp. 178–193, 2017.

[6] K. Shankar, A. R. W. Sait, D. Gupta, S. Lakshmanaprabu, A. Khanna, and H. M. Pandey, "Automated detection and classification of fundus diabetic retinopathy images using synergic deep learning model," *Pattern Recognition Letters*, vol. 133, pp. 210–216, 2020.

[7] S. Akbar, M. U. Akram, M. Sharif, A. Tariq, and U. ullah Yasin, "Arteriovenous ratio and papilledema based hybrid decision support system for detection and grading of hypertensive retinopathy," *Computer methods and programs in biomedicine*, vol. 154, pp. 123–141, 2018.

[8] Q. Abbas and M. E. Ibrahim, "Densehyper: an automatic recognition system for detection of hypertensive retinopathy using dense features transform and deep-residual learning," *Multimedia Tools and Applications*, vol. 79, no. 41, pp. 31 595–31 623, 2020.

[9] L. Zhang, M. Yuan, Z. An, X. Zhao, H. Wu, H. Li, Y. Wang, B. Sun, H. Li, S. Ding *et al.*, "Prediction of hypertension, hyperglycemia and dyslipidemia from retinal fundus photographs via deep learning: A cross-sectional study of chronic diseases in central china," *PloS one*, vol. 15, no. 5, p. e0233166, 2020.

[10] B. Dashtbozorg, A. M. Mendonça, and A. Campilho, "An automatic graph-based approach for artery/vein classification in retinal images," *IEEE Transactions on Image Processing*, vol. 23, no. 3, pp. 1073–1083, 2014.

[11] X. Xu, W. Ding, M. D. Abràmoff, and R. Cao, "An improved arteriovenous classification method for the early diagnostics of various diseases in retinal image," *Computer methods and programs in biomedicine*, vol. 141, pp. 3–9, 2017.

[12] R. Estrada, M. J. Allingham, P. S. Mettu, S. W. Cousins, C. Tomasi, and S. Farsiu, "Retinal artery-vein classification via topology estimation," *IEEE Transactions on Medical Imaging*, vol. 34, no. 12, pp. 2518–2534, 2015.

[13] O. Ronneberger, P. Fischer, and T. Brox, "U-net: Convolutional networks for biomedical image segmentation," in *International Conference on Medical image computing and computer-assisted intervention*. Springer, 2015, pp. 234–241.

[14] M. Z. Khan and Y. Lee, "Localization of ocular vessels with context sensitive semantic segmentation," in *2021 IEEE EMBS International Conference on Biomedical and Health Informatics (BHI)*, 2021, pp. 1–5.

[15] Z. Gu, J. Cheng, H. Fu, K. Zhou, H. Hao, Y. Zhao, T. Zhang, S. Gao, and J. Liu, "Ce-net: Context encoder network for 2d medical image segmentation," *IEEE transactions on medical imaging*, vol. 38, no. 10, pp. 2281–2292, 2019.

[16] O. Oktay, J. Schlemper, L. L. Folgoc, M. Lee, M. Heinrich, K. Misawa, K. Mori, S. McDonagh, N. Y. Hammerla, B. Kainz *et al.*, "Attention u-net: Learning where to look for the pancreas," *arXiv preprint arXiv:1804.03999*, 2018.

[17] Z. Zhou, M. M. R. Siddiquee, N. Tajbakhsh, and J. Liang, "Unet++: Redesigning skip connections to exploit multiscale features in image segmentation," *IEEE Transactions on Medical Imaging*, vol. 39, no. 6, pp. 1856–1867, 2020.

[18] L. Li, M. Verma, Y. Nakashima, H. Nagahara, and R. Kawasaki, "Iternet: Retinal image segmentation utilizing structural redundancy in vessel networks," in *Proceedings of the IEEE/CVF Winter Conference on Applications of Computer Vision*, 2020, pp. 3656–3665.

[19] L. Li, M. Verma, Y. Nakashima, R. Kawasaki, and H. Nagahara, "Joint learning of vessel segmentation and artery/vein classification with post-processing," in *Medical Imaging with Deep Learning*. PMLR, 2020, pp. 440–453.

[20] J. Staal, M. D. Abràmoff, M. Niemeijer, M. A. Viergever, and B. Van Ginneken, "Ridge-based vessel segmentation in color images of the retina," *IEEE transactions on medical imaging*, vol. 23, no. 4, pp. 501–509, 2004.

[21] A. Budai, R. Bock, A. Maier, J. Hornegger, and G. Michelson, "Robust vessel segmentation in fundus images," *International journal of biomedical imaging*, vol. 2013, 2013.

[22] M. M. Fraz, P. Remagnino, A. Hoppe, B. Uyyanonvara, A. R. Rudnicka, C. G. Owen, and S. A. Barman, "An ensemble classification-based approach applied to retinal blood vessel segmentation," *IEEE Transactions on Biomedical Engineering*, vol. 59, no. 9, pp. 2538–2548, 2012.

[23] T. Laibacher, T. Weyde, and S. Jalali, "M2u-net: Effective and efficient retinal vessel segmentation for real-world applications," in *Proceedings of the IEEE/CVF Conference on Computer Vision and Pattern Recognition Workshops*, 2019, pp. 0–0.

[24] A. Hoover, V. Kouznetsova, and M. Goldbaum, "Locating blood vessels in retinal images by piecewise threshold probing of a matched filter response," *IEEE Transactions on Medical imaging*, vol. 19, no. 3, pp. 203–210, 2000.

[25] S. Holm, G. Russell, V. Nourrit, and N. McLoughlin, "Dr hagis—a fundus image database for the automatic extraction of retinal surface vessels from diabetic patients," *Journal of Medical Imaging*, vol. 4, no. 1, p. 014503, 2017.

[26] R. Estrada, M. J. Allingham, P. S. Mettu, S. W. Cousins, C. Tomasi, and S. Farsiu, "Retinal artery-vein classification via topology estimation," *IEEE transactions on medical imaging*, vol. 34, no. 12, pp. 2518–2534, 2015.

[27] J. I. Orlando, J. B. Breda, K. Van Keer, M. B. Blaschko, P. J. Blanco, and C. A. Bulant, "Towards a glaucoma risk index based on simulated hemodynamics from fundus images," in *International Conference on Medical Image Computing and Computer-Assisted Intervention*. Springer, 2018, pp. 65–73.

[28] J. Zhang, B. Dashtbozorg, E. Bekkers, J. P. Pluim, R. Duits, and B. M. ter Haar Romeny, "Robust retinal vessel segmentation via locally adaptive derivative frames in orientation scores," *IEEE transactions on medical imaging*, vol. 35, no. 12, pp. 2631–2644, 2016.

[29] P. Liskowski and K. Krawiec, "Segmenting retinal blood vessels with deep neural networks," *IEEE transactions on medical imaging*, vol. 35, no. 11, pp. 2369–2380, 2016.

[30] H. Fu, Y. Xu, S. Lin, D. W. K. Wong, and J. Liu, "Deepvessel: Retinal vessel segmentation via deep learning and conditional random field," in *International conference on medical image computing and computer-assisted intervention*. Springer, 2016, pp. 132–139.

[31] L. Gu, X. Zhang, H. Zhao, H. Li, and L. Cheng, "Segment 2d and 3d filaments by learning structured and contextual features," *IEEE transactions on medical imaging*, vol. 36, no. 2, pp. 596–606, 2016.

[32] J. I. Orlando, E. Prokofyeva, and M. B. Blaschko, "A discriminatively trained fully connected conditional random field model for blood vessel segmentation in fundus images," *IEEE transactions on Biomedical Engineering*, vol. 64, no. 1, pp. 16–27, 2016.

[33] Z. Yan, X. Yang, and K.-T. Cheng, "Joint segment-level and pixel-wise losses for deep learning based retinal vessel segmentation," *IEEE Transactions on Biomedical Engineering*, vol. 65, no. 9, pp. 1912–1923, 2018.

[34] X. Wang, X. Jiang, and J. Ren, "Blood vessel segmentation from fundus image by a cascade classification framework," *Pattern Recognition*, vol. 88, pp. 331–341, 2019.

[35] M. Z. Alom, C. Yakopcic, M. Hasan, T. M. Taha, and V. K. Asari, "Recurrent residual u-net for medical image segmentation," *Journal of Medical Imaging*, vol. 6, no. 1, p. 014006, 2019.

[36] S. Y. Shin, S. Lee, I. D. Yun, and K. M. Lee, "Deep vessel segmentation by learning graphical connectivity," *Medical image analysis*, vol. 58, p. 101556, 2019.

[37] J. Zhuang, "Laddernet: Multi-path networks based on u-net for medical image segmentation," *arXiv preprint arXiv:1810.07810*, 2018.

[38] L. Mou, L. Chen, J. Cheng, Z. Gu, Y. Zhao, and J. Liu, "Dense dilated network with probability regularized walk for vessel detection," *IEEE transactions on medical imaging*, vol. 39, no. 5, pp. 1392–1403, 2019.

[39] Z. Zhuo, J. Huang, K. Lu, D. Pan, and S. Feng, "A size-invariant convolutional network with dense connectivity applied to retinal vessel segmentation measured by a unique index," *Computer methods and programs in biomedicine*, vol. 196, p. 105508, 2020.

[40] H. Zhao, H. Li, and L. Cheng, "Improving retinal vessel segmentation with joint local loss by matting," *Pattern Recognition*, vol. 98, p. 107068, 2020.

[41] N. Liu, L. Liu, and J. Wang, "Local adaptive u-net for medical image segmentation," in *2020 IEEE International Conference on Bioinformatics and Biomedicine (BIBM)*. IEEE, 2020, pp. 670–674.

[42] A. Galdran, M. Meyer, P. Costa, A. Campilho *et al.*, "Uncertainty-aware artery/vein classification on retinal images," in *2019 IEEE 16th International Symposium on Biomedical Imaging (ISBI 2019)*. IEEE, 2019, pp. 556–560.

[43] R. Hemelings, B. Elen, I. Stalmans, K. Van Keer, P. De Boever, and M. B. Blaschko, "Artery–vein segmentation in fundus images using a fully convolutional network," *Computerized Medical Imaging and Graphics*, vol. 76, p. 101636, 2019.